V International Conference on Computational Methods for Coupled Problems in Science and Engineering
COUPLED PROBLEMS 2013
S. Idelsohn, M. Papadrakakis and B. Schrefler (Eds)

A COUPLED THERMO-ELECTRICAL PROBLEM FOR THE OPTIMIZATION OF RADIO FREQUENCY ABLATION TREATMENTS

ALESSANDRO FORMISANO, FABRIZIO FERRAIOLI AND RAFFAELE MARTONE

Dipartimento di Ingegneria Industriale e dell'Informazione
Seconda Università DEGLI Studi di Napoli
Via Roma 29, Aversa (CE), Italy
Email: Raffaele.Martone@unina2.it

Key words: Coupled Problems, Multiphysics Problems, Biomedical applications, Numerical electromagnetic computation, Optimization methods

Abstract. Clinical treatment of some forms of epathocarcinoma makes use, under certain circumstances, of thermal ablation induced by radio frequency currents injected into the tumor volume. The success of the operation relies upon the capability of totally ablating the tumor volume simultaneously preventing healthy tissue damage and skin burns due to the ground pad heating. Such a treatment is liable to possible improvements if a mathematical model is available, and a suitable numerical optimization procedure is adopted. The problem falls in the class of strongly coupled problems; as matter of fact the thermal diffusion is linked to the electrical current conduction through the main heat source which is the Ohmic power density while, in addition, the current conduction is linked to the thermal dynamics being the electrical resistivity a function of the thermal map itself.
In this paper, a FEM based numerical model for radio frequency ablation of liver tumors is considered and its optimization is addressed with optimal planning, imposing non linear partial differential equation of the model as a constraint in a space state; in addition, the coupling aspects are highlighted and discussed.

1 INTRODUCTION

Radio Frequency Ablation (RFA) is a treatment for some forms of liver tumors, based on the local deposition of Ohmic power by injection of radiofrequency currents though suitably designed probes inserted into patient's abdomen [1, 2]. A typical RFA session requires the laparoscopical or percutaneous insertion of a probe into the ill tissue, the positioning of the probe tip into the tumor, the application of a single or multiple return electrode, usually on the back of the patient [3, 4], and, finally, the injection of RF current through a specific power supply system. Note that the probe tip is a rather sophisticated device, eventually endowed with a cooling water flow and metallic retractable prongs designed to operate in electric contact with the tumor [5].

The Ohmic power deposition produces a heat source whose intensity depends on the current density and tissues conductivity. The Ohmic power density combines with other heat sources, such as metabolic heat generation, and with heat sinks, such as blood perfusion, to determine the temperature evolution in the tumor and adjacent regions. The RFA process is designed to determine a net temperature increase inside the tumor high enough to lead tumor cells to necrosis avoiding tissue carbonization. in addition, the ideal goal of the treatment is to achieve the necrosis exclusively in the tumor volume in as few sessions as possible [5, 2].

The mathematical modeling requires several equations falling in different technical fields: (i) a thermal non linear, dynamic diffusion equation; (ii) a stationary ac current equation; (iii) a non linear, integral equation to describe the cellular necrosis. Further equations can be required to represent additional elements as the electrical circuit powering the process. Finally, to look for a favorable solution, an additional non linear optimization function is used and its minimum is sought. Due to the interaction among the equations, the problem has to be faced by means of a well suited coupled problem approaches.

The time evolution of the temperature map and the consequent tissues damage index depend on a number of parameters, many of them either only partially known (such as thermal and electrical tissues conductivities), or not under the control of the surgeon (such as the patient's physiological reaction to the heat deposition). A number of papers were published about possible improvements to the basic protocol [2, 3, 4, 5]. In particular, non linear programming methods have been introduced as a valuable tool to approach the problem; it has also been highlighted that the use of multiple return pads can be used to suitably control the shape of the isothermal surfaces in order to prevent possible damage to healthy tissue [6, 7, 8], or that the use of multi-prong probes could improve the heat deposition in the tumor, while preserving adjacent tissues from excessive damages.

This paper proposes a novel and more general formulation for the optimization of the current waveforms in the RFA electrodes, based on optimal planning theory [9, 10]. The advantages achievable in terms of the effectiveness are assessed by using a suitable numerical model of the human body specifically developed for this application.

In sect. II the problem formulation is presented and the coupling aspects highlighted; in Sect. III a numerical example is presented to demonstrate the effectiveness of the approach; in addition, a comparison of the optimal planning of the classical monopolar heating and of an innovative multipolar structure is discussed; in Sect. IV an example of waveforms optimization is presented; finally, in Sect. V some conclusions are drawn.

2 MATHEMATICAL MODEL

The forward operator describing RFA dynamics is first briefly presented in section 2.1, and then some details about its Finite Element (FE) discretized version are given in section 2.2. The optimization strategy, the treatment of the differential constraints, required to treat the model in the context of the optimal planning algorithms [9], as well as the choice of degrees of freedom (DOF), are discussed in section 2.3.

2.1 Forward Problem: Electro-thermal dynamics of RFA

The mathematical model describing the temperature map evolution during RFA treatments (forward problem) falls in the coupled electro-thermal problem class, including two suitably coupled electromagnetic and thermal sub-models.

In the electromagnetic sub-problem, the Ohmic power density distribution is calculated, by assuming that the electrical properties of the tissue are known as well as the values of RF currents applied through inner needle-shaped electrodes and one or more outer return pads.

$$\begin{cases} \nabla\cdot\left(\sigma\nabla\varphi(\boldsymbol{r},t)+\varepsilon\partial_t\nabla\varphi(\boldsymbol{r},t)\right)=0 & in\ \Omega \\ \int\limits_{\Gamma_{elec(k)}} \mathbf{j}_s(\boldsymbol{r},t)\cdot d\mathbf{S}=I_k(t) & k\in\{1,2,...,N_E\} \\ \varphi(\boldsymbol{r},t)=0 & on\ \partial\Omega_{ref.prong} \\ \left(\sigma\nabla\varphi(\boldsymbol{r},t)+\varepsilon\partial_t\nabla\varphi(\boldsymbol{r},t)\right)\cdot\hat{\boldsymbol{n}}=0 & on\ \partial\Omega_{skin} \end{cases} \quad (1)$$

where Ω is the analysis domain (typically, the patient's torso), $\boldsymbol{r}$ is the position vector in Ω, σ is the electrical conductivity, ε the electrical permittivity, ϕ is the electric scalar potential.

In this paper a multiple-prongs probe, with electrically independent elements, is assumed [7], and one of the prongs is supposed at system ground potential; different currents are then imposed in the remaining prongs as well as in the external (multiple) return pads, obtaining a flexible "multipolar" probe system. Consequently, $\partial\Omega_{ref.\ prong}$ is the surface of the prong where the reference (electric scalar) potential is applied, $\partial\Omega_{elec(k)}$, k=1,2 … N_E, are patches modelling both the external and internal electrodes, and $\partial\Omega_{skin}$ is the patient's skin not covered by electrodes.

The electromagnetic sub-problem is coupled to the thermal one through the resistivity ($\rho=1/\sigma$), because of its temperature-dependance:

$$\rho(\mathbf{r}, f, T) = \rho_0(\mathbf{r}, f)\left[1+\beta\left(T-T_{ref}\right)\right] \tag{2}$$

where T_{ref} is a reference temperature. In general the conductivity depends also on the working frequency.

The tissues temperature evolution during RFA is described by the Pennes's bioheat model [11]

$$\begin{cases} mc\dfrac{\partial T(\mathbf{r},t)}{\partial t} = \nabla\bullet k\nabla T(\mathbf{r},\mathrm{t}) + p_0(\mathbf{r},\mathrm{t}) - p_{bl}(\mathbf{r},\mathrm{t}) & in\ \Omega \\ k\dfrac{\partial T(\mathbf{r},t)}{\partial n} = h_{conv}\left(T(\mathbf{r},t) - T_\infty(\mathbf{r})\right) & on\ \partial\Omega - \partial\Omega_{probe} \\ T(\mathbf{r},t) = T_{cooling} & on\ \partial\Omega_{probe} \\ T\left(\mathbf{r},0^-\right) = T_0(\mathbf{r}) & in\ \Omega \end{cases} \tag{3}$$

where $p_O(\mathbf{r},\mathrm{t})$ is the Ohmic power density (in this case metabolic heat sources are neglected), $p_{bl} = h_{bl}\,[T(\mathbf{r},t)-T_{bl}]$ is the tissue perfusion, $T_{cooling}$ is the temperature of the internal (cooled) probe, and suitable natural convection boundary conditions are imposed on the remaining part of domain boundary. In addition, m is the tissue mass density, c the tissue specific heat, k the thermal conductivity, $h_{bl} = m_{bl}\,c_{bl}\,w_{bl}$ the convective heat transfer coefficient accounting for the blood perfusion (m_{bl} is the blood mass density, c_{bl} the blood specific heat, w_{bl} the blood perfusion coefficient), T_{bl} is the temperature of blood, h_{conv} is the convective coefficient, T_∞ is the bulk temperature, and T_0 is the temperature map at $t=0^-$.

In a coupled problems the complete set of equations in the mathematical model should be simultaneously faced at all the time steps and in all space points relevant for the analysis. As a consequence, the computing burden required for high accuracy evaluations, could be not compatible with many of the present computer performance.

Fortunately sometimes the actual dependence of some coefficient on the exchange variables (e.g. temperature from thermal analysis to determine conductivity in electromagnetic analysis, or Ohmic power density from electromagnetic to thermal analyses) is as weak to be neglected within the margins of the computation accuracy; in addition, sometime the time scale of the coupled equations can be so different to allow freezing, within the accuracy bar, a phenomenon while the others reach their steady state.

Therefore, in the solution of coupled dynamical system a preliminary analysis of the origins of the coupling (and their consistency) together with the comparison of the typical time scales, is strongly recommended because of the beneficial effects in the reduction of the computational burden.

In the case at hand it is easy to find a number of important simplifications:

S1. The time scale of thermal diffusion is in the order of hundreds of s, much longer then the electromagnetic one, in the order of fraction of μs.

S2. Except for conductivity and perfusion coefficients, all the dependences of the model coefficients

on the temperature are negligible because falls within the error bar of the schematization [2].

Then two consequences follow:

CS1. the current can be considered in AC steady state; then (i) the current can be studied in the complex phasor domain; (ii) in the optimization procedure, the currents can be represented by just the simple complex representation; (iii) the transient electrical effects can be neglected in the thermal dynamic studies;

CS2. the coupling between thermal and electrical models can be assumed concentrated in the impact of the temperature on conductivity coefficient;

Here, as additional hypothesis, well met in typical applications,

CS3. the circuit sources are assumed "current controlled" and then not depending on the resistances.

According to the fist simplification, the electromagnetic equations (1) can be written in the complex phasor domain

$$\begin{cases} \nabla \cdot \left(\dot{\gamma} \nabla \tilde{\varphi}(\boldsymbol{r}) \right) = 0 & in\,\Omega \\ \int\limits_{\Gamma_{elec(k)}} \tilde{\mathbf{j}}_s(\boldsymbol{r}) \cdot \mathrm{d}\mathbf{S} = \tilde{\mathrm{I}}_{\mathrm{k}} & k \in \{1,2,...,N_E\} \\ \tilde{\varphi} = 0 & on\ \partial\Omega_{ref.prong} \\ \dot{\gamma} \dfrac{\partial \tilde{\varphi}}{\partial n} = 0 & on\ \partial\Omega_{skin} \end{cases} \tag{4}$$

where $\dot{\boldsymbol{\gamma}}(\boldsymbol{r}, f, T) = \sigma(\boldsymbol{r}, f, T) + \mathrm{j}2\pi f \varepsilon(\boldsymbol{r}, f)$ is the complex electrical admittivity profile at working frequency f, $\tilde{\boldsymbol{\varphi}}$, $\tilde{j}_{\mathrm{k}}, \tilde{\mathrm{I}}_{\mathrm{k}}$ are the (phasor) electric scalar potential, current density and electrode currents, respectively.

It should be noticed that (4) is able to provide the thermal Ohmic power p_0 as $p_O(\mathbf{r}, \mathrm{t}) = Real\{\tilde{\mathbf{E}}(\mathbf{r}, \omega) \cdot \tilde{\mathbf{J}}^*(\mathbf{r}, \omega)\}/2$ (where $\tilde{\mathbf{E}}(\mathbf{r}, \omega)$ is the phasor electric field map and "*" denotes the complex conjugate) or, equivalently $p_0 = E^2/(2\,\sigma)$.

According to (1), the input variables are the complex current patterns $\hat{\boldsymbol{I}}$ applied to the internal and external electrodes (the DOF of the optimization problem), and the initial thermal map $T_0(\boldsymbol{r})$. The time evolution of the model can be carried out by means of several approaches, including Runge-Kutta, predictor-corrector and so on. Here, a fixed time step algoritm has been used because it is able to provide a fast resolution of the optimization problem while guaranteeing the required accuracy.

The output of the model are the thermal map $T(\boldsymbol{r},t)$ in the patient's torso during RFA treatment. For the sake of simplicity, in the inverse problem, the forward operator will be synthetically indicated as $\mathcal{F}(\hat{\boldsymbol{I}}, T_0)$, whewre $\mathcal{F}: (\hat{\boldsymbol{I}}, T_0) \rightarrow T(\boldsymbol{r},t)$.

2.2 Finite Elements Model of the Torso

The 3D solution domain Ω here used for the following numerical simulations is shown in Fig.1. It represents a rather simplified human torso, with a RFA probe inserted into the liver, and with multiple return pads. The main simplifying assumption is that only three different tissues were considered,

denoted in the following by “liver”, “torso” and “tumor”, characterized by different values of electromagnetic and thermal properties.

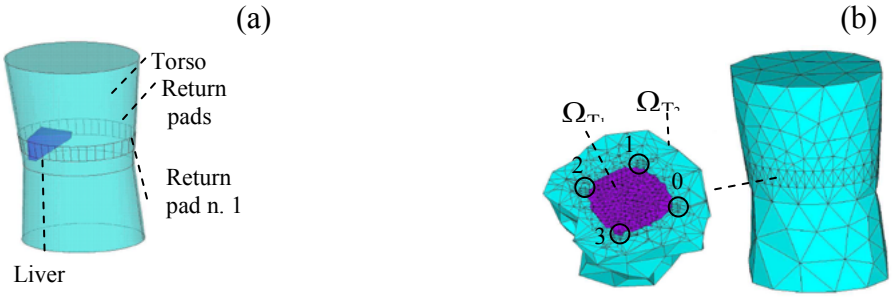

Figure 1: (a) 3D Model of the torso Ω and (b) FE mesh used in the calculations, including the detail of the target region of the RFA treatment and of the internal probe prongs

FE resolution of coupled problem (1)-(3) provides a discrete version F of the operator $\mathfrak{F}$ transforming the input couple $(\hat{\boldsymbol{I}}, T_0)$ into the sequence of nodal temperatures array $\mathbf{T}_n(t_k)$ with k = 1, 2, …. N_s, where N_s is the number of time steps.

2.3 Optimal Planning of RFA Treatment

Optimal planning of RFA treatment introduces a schedule in the heating of the various regions, compatible with the possible system dynamics, by modifying current amplitudes within values safe for human treatments (denoted from now on as Feasible Current Patterns, FCP). If a “desired” time varying temperature map $T^{des}(\mathbf{r},t)$ is assigned, the optimal planning problem can be formulated as that of finding the sequence of current pattern $\hat{\mathbf{I}}_{\min}$ such that the following error functional is minimized:

$$\mathscr{E}(\hat{\mathbf{I}},T_0)=\left\|W(\mathbf{r},t)\left(T^{des}(\mathbf{r},t)-\mathfrak{F}\left(\hat{\mathbf{I}},T_0\right)\right)\right\|^2_{L^2}+\alpha(t)\left\|\hat{\mathbf{A}}\hat{\mathbf{I}}\right\|^2_{L^2}\quad \forall t\geq 0 \tag{5}$$

where W is a weighting function, α is regularization parameter and $\hat{\mathbf{A}}$ is current pattern preconditioning matrix. The minimization of error functional (5) is subject to equations (1)-(3) as equality constraints and, as an additional constraint, $\hat{\mathbf{I}}$ is taken as bounded by the set of FCP.

The minimization of (5) is intended for every time t. Thanks to the FE discretization of the forward operator, the problem (5) is expressed in a discretized version. If limiting to a single step in the thermal transient analysis, (5) can be written in a time and space discretized version:

$$E\left(\hat{\mathbf{I}}_k,\mathbf{T}_0\right)=\left\|\left(\mathbf{T}_k^{des}-\boldsymbol{F}_k(\hat{\mathbf{I}}_k,\mathbf{T}_0)\right)\mathbf{W}_k^T\left(\mathbf{T}_k^{des}-\boldsymbol{F}_k(\hat{\mathbf{I}}_k,\mathbf{T}_0)\right)\right\|^2+\alpha_k\left\|\hat{\mathbf{A}}_k\hat{\mathbf{I}}_k\right\|^2\quad \forall k\in\{0,\ldots,N_s\} \tag{6}$$

where k denotes the time step, $\boldsymbol{F}_k(\hat{\mathbf{I}}_k,\mathbf{T}_0)$ is the array of calculated temperature in the centroid of the elements mesh, $\mathbf{T}_k^{des}$ is the corresponding "desired" value, $\mathbf{W}_k$ is a wheigthing array and α_k is is the reguralization parameter and “T” denotes transposition of an array. Notice that the weighting function/array accounts for the "importance" of the requirements in each subregions of the solution domain Ω.

This approach represents a generalization of what presented in [6,7,8]: the introduction of the new independent prong currents provides improved effectiveness and flexibility to ablation process.

3. NUMERICAL EXAMPLE

In this section, the advantages of the two innovative aspects of RFA planning are demonstrated in the numerical case described in Sect. 1.2. First, independent current sources for the probe prongs (and for the return pads) are used to achieve a better temperature control in the tumor region, and then current waveforms in prongs and pads are optimized to improve spatial uniformity Ohmic power deposition.

The following geometrical data have been assumed. The tumor region Ω_T, Fig. 1, is a sphere of radius 15 mm, split into two "target" regions for RFA: Ω_{T1} (radius 7 mm) and Ω_{T2} (internal radius 7mm, external radius 15 mm). Probe prongs have been modeled as cylindrical cavities (radius 1mm, length 10 mm, centroids lying on a circle with 7.5 mm radius, equally spaced) encircled in Fig.1b.

The FE mesh includes 33282 1st order tetrahedral elements and 5740 nodes (see Fig. 1).

The first point is assessed by applying a single current between a single return pad (number 1 in Fig. 1(a)) and the whole set of prongs of the internal probe, assumed as equipotential (Single Current Optimization, SCO). Prong 0 (see Fig.1(b)) is then grounded, while the remaining ones are supposed to be supplied each with a different current and zero current in the return pads has been imposed (Multiple Current Optimization, MCO). A time interval of 100s has been considered for a first part of a possible RFA process, and subdivided in five subinterval 20 s each long, to actuate the step by step optimization process. The desired uniform temperature sequences T^{dR1}=[37.6, 38.2, 38.8, 39.4, 40] °C and T^{dR2}=[37.4, 37.8, 38.2, 38.6, 39] °C are assumed in (6) for the five time steps in the two controlled region, respectively.

The current to be optimized are sinusoidal functions characterized by the same frequency of f=450 kHz and amplitudes and phases as degrees of freedom. For the sake of simplicity all the phases of external currents I_K are supposed vanishing and just the amplitudes have been included in the optimization search. In both cases, SCO and MCO, a deterministic approach has been applied (golden search and parabolic interpolation in SCO and pattern search in MCO); a starting value of 0.2 A for each unknown has been assumed at the first time step while the optimum found in the previous, has been fixed for starting in the following steps.

In addition, an absolute FCP constraint of 0.6 A has been imposed of the current in SCO, while the constraint for each currents in MCO has been fixed at 0.3 A. Finally, tissue properties and perfusion data used in the simulation are reported in Table I.

Table I: Main tissue properties and perfusion data used in the simulations

	σ [S/m]	ε_r	k [W/m °C]	M [Kg/m^3]	c [J/Kg°C]	W_{bl} [kg/(sm^3)]
Liver	0.33	2700	0.51	1060	3600	16.7
Torso	0.25	2700	0.51	1060	3500	0.6

The results of the optimization are summarized in Fig. 2. In order to evaluate the effectiveness of the process, the uniformity of the temperature within the control domain should be considered; then the percentage of the volume in TR_1 and TR_2 characterized by a temperatures within the ±5% of the desired values have been computed.

The results (Fig. 3) clearly show the effectiveness of the multiple independent prong currents in the ablation process.

Figure 2: Sequences of optimal current patterns for MCO (a) and for multipolar control of the internal probe SCO (b)

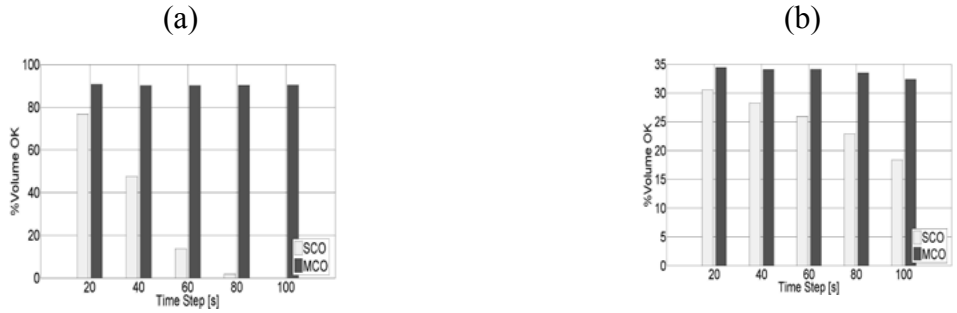

Figure 3: Comparison of percentage of volume where the temperature is close to the scheduled for TR_1 (a) and for TR_2 (b) respectively

This encouraging results is fully confirmed by the temperature map (see Fig. 4 for the profile at 100 s) in the both the domains TR_1 and TR_2 showing an occurrence of joining hot spots, especially in TR_1, when a MCO is performed.

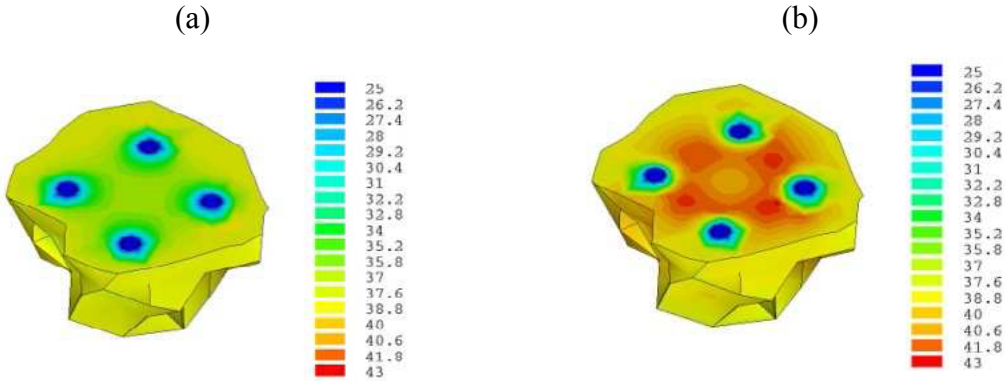

Figure 4: Local temperature maps in the case of equipotential internal prongs (a) and in the case of multipole control of the prongs (b) at t=100 s.

Finally, the marginal role of the external pads has been assessed. The effectiveness of the system with four internal prongs with and without an additiona external pad have been compared: the difference is very small and the current in the external pad is, in any case, within the limit of a few percentages of the internal currents.

4. CONCLUSIONS

In this paper the effectiveness of prongs as independent electrodes in ablation procedures for clinical treatment of liver tumors has been discussed.

Of course, further careful analysis are required to assess the actual feasibility of the method. Particular attention should be devoted to the maximum differential currents that can be imposed on prongs and on maximum frequencies to prevent the capacitive couplings among prongs.

Unfortunately the important uncertainties affecting living tissue parameters and geometrical information of the organs, prevent to obtain results so reliable and accurate to be directly applied in a clinical RFA protocol. For this reason, the outcome of the simulations must be taken as a suggestion than as a prescription. However their value remain very important in looking for the most effective ablation treatments.

Some interesting global properties coming out of the study here performed are finally listed:

- the marked superiority of the multipolar control of the probe prongs in terms of ablation capability emerges, when compared to monopolar prongs excitation and use of external return pads. This is in full agreement with the previous theoretical and experimental investigations [1];
- the optimal way to concentrate Ohmic power density in the target regions is characterized by an almost symmetric system of AC currents, in phase opposition according with the space distribution, in such a way to exhibit a "strong" interaction among opposite prongs.

REFERENCES

[1] Lencioni, R., Cioni, D., Crocetti, L. and Bartolozzi, C. Percutaneous Ablation of Hepatocellular Carcinoma: State-of-the-Art. *Liver Transplantation* (2004), **10**: S91–S97.

[2] Chen, C. R. and Miga, M. I. Optimizing Electrode Placement Using Finite-Element Models in Radiofrequency Ablation Treatment planning, *IEEE Trans. on Biomed. Eng.*, (2009) **56**: 237-245.

[3] Rhim, H. et al. Radiofrequency Thermal Ablation of Abdominal tumors: Lessons Learned from Complications *Radiographics*, (2004) **24**: 41-53.

[4] Schutt, D. J. and Haemmerich, D. Sequential Activation of a Segmented Ground Pad, *IEEE Trans. on Biom. Eng.* (2008) **55**: 1881-1889.

[5] Haemmerich, D., Staelin, S. T., Tungjitkusolmun, S., Lee, F. T., Mahvi, D.M. and Webster, J. G. Hepatic Bipolar Radio-Frequency Ablation Between Separated Multiprong Electrodes *IEEE Trans. on Biom. Eng.* (2001) **48**: 1145-1152.

[6] Caminiti, I.M.V., Ferraioli, F., Formisano, and Martone, R. Adaptive Ablation Treatment Based on Impedance Imaging. *IEEE Trans. on Mag.*, (2010) **46**: 3329-3332.

[7] Ferraioli, F., Formisano, A., Martone, R. Optimizing the Electrothermal Dynamics in Radio Frequency Ablation Treatments, *Proc. of Compumag 2011*, *Sydney, Australia*, (2011).

[8] Caminiti, I.M.V., Ferraioli, F., Formisano, A. and Martone, R. Three Dimensional Optimal Current Patterns For Radiofrequency Ablation Treatments. *Compel,* (2012) **31**: 985-995.

[9] LaValle, S. M. *Planning algorithms*. Cambridge University Press, (2006).

[10] Luenberger, D. G. *Introduction to Dynamic Systems: Theory, Models, and Applications*. Wiley, (1979).

[11] Wissler, E. H. Pennes' 1948 Paper Revisited. *J. Appl. Physiol.* (1998) **85**: 35-41.